Al_2O_3 corundum (IVCT) supplemental figures and data

1) Corundum GRR 1334 from Malacacheta, Brazil

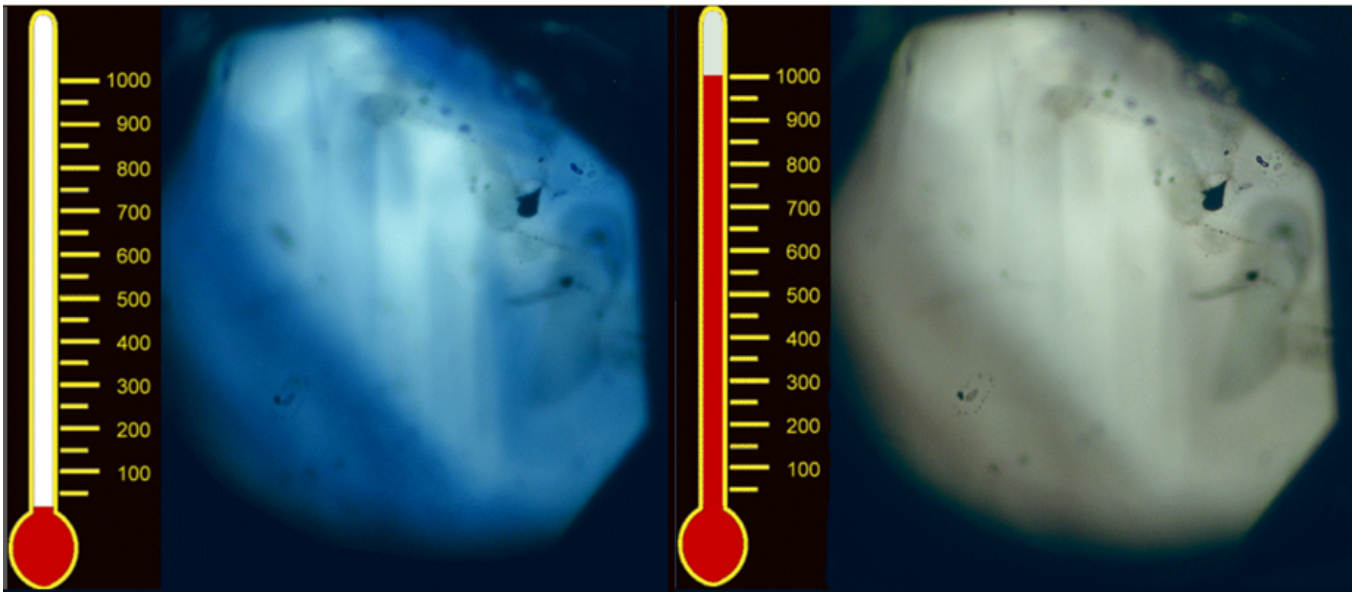

Supplemental Figure 1. Photos of a blue sapphire from Malacacheta, Minas Gerais, Brazil, at 23 °C and 1000 °C. The blue color at room-temperature is lost at elevated temperatures but returns when the sample is cooled.

2) Corundum GRR 3473-YS-D from Queensland, Australia

Supplemental Table 2. Parameters for Gaussian components compatible with IVCT assignments in GRR3473-YS-D Corundum.

	19 °C Start	17 °C End	1000 °C Heat
Center (cm^{-1})	17843	17934	17008
Center (nm)	560.44	557.61	587.96
Linear intensity	0.2148	0.1916	0.0779
Integral intensity	1161	1043	402
FWHM (cm^{-1})	5078	5113	4851
Center (cm^{-1})	13927	13950	14243
Center (nm)	718.04	716.84	702.08
Linear intensity	0.1098	0.1009	0.0172
Integral intensity	375	347	49
FWHM (cm^{-1})	3210	3230	2680
Center (cm^{-1})	11036	10928	10942
Center (nm)	906.11	915.11	913.92
Linear intensity	0.0431	0.0561	0.0212
Integral intensity	140	188	80
FWHM (cm^{-1})	3055	3144	3557

3) Corundum GRR 2382-B from Yogo Gulch, Judith Basin County, Montana.

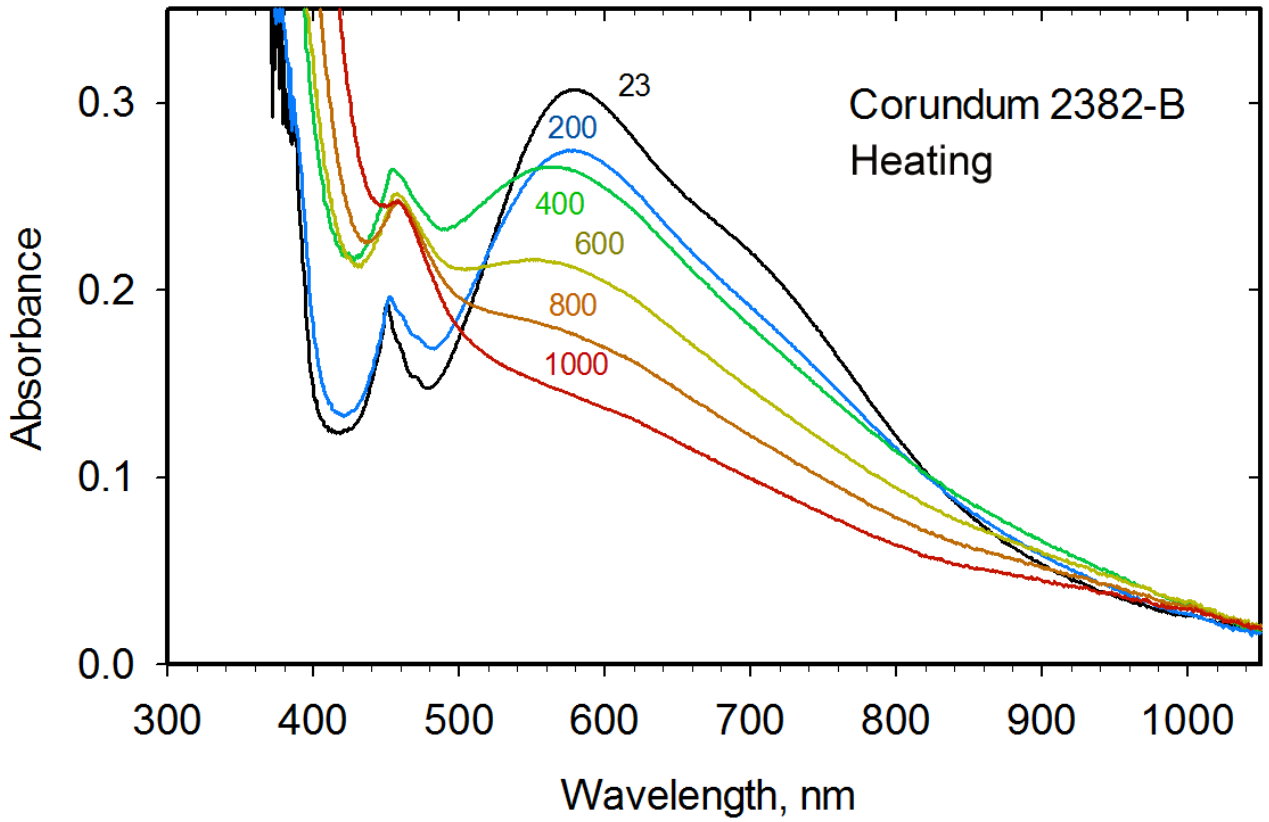

Supplemental Figure 3a. Initial heating run of GRR2382-B corundum from Yogo Gulch, Montana, presented as 1.000 mm thick. Features at both short and long wavelengths increase during heating from 23 °C to 1000 °C.

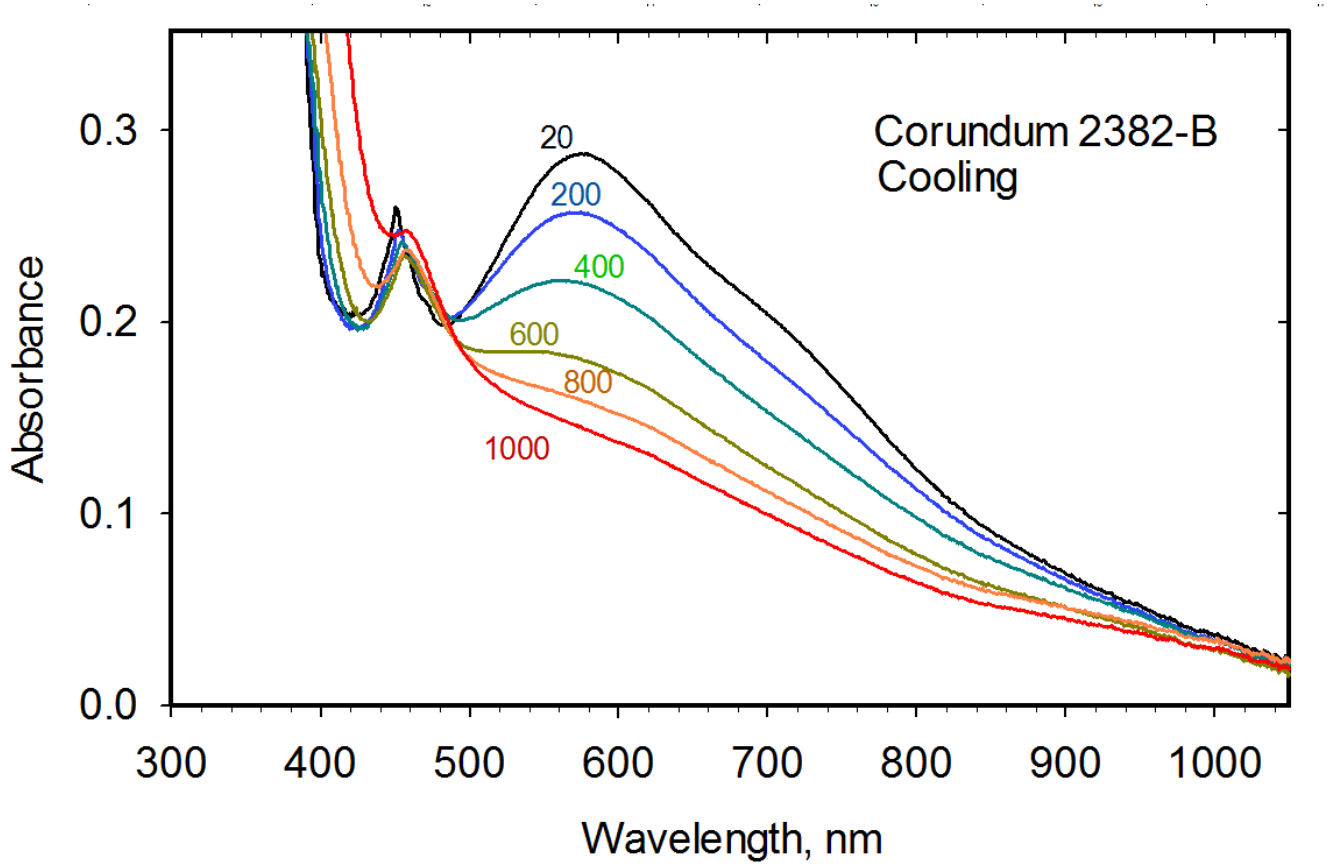

Supplemental Figure 3b. Initial cooling run of GRR2382-B corundum from Yogo Gulch, Montana, presented as 1.000 mm thick. The increase in intensity during the initial heating run of the absorption features at short and long wavelengths is retained during cooling from 1000 °C to 20 °C.

Supplemental Table 3. Gaussian components for selected bands at room temperature, 500 °C, and 1000 °C in GRR2382-B corundum.

	24 °C Start	500 °C Heat	1000 °C Heat
Center (cm^{-1})	20490	19409	20685
Center (nm)	488.04	515.22	483.45
Linear intensity	0.0646	0.1709	0.1637
Integral intensity	178	858	1011
FWHM (cm^{-1})	2594	4714	5804
Center (cm^{-1})	17401	16959	16177
Center (nm)	574.67	589.66	618.18
Linear intensity	0.2867	0.0736	0.0936
Integral intensity	1648	246	439
FWHM (cm^{-1})	5400	3148	4408
Center (cm^{-1})	14134	14625	14154
Center (nm)	707.49	683.78	706.5
Linear intensity	0.0655	0.1227	0.0163
Integral intensity	187	518	40
FWHM (cm^{-1})	2685	3971	2274
Center (cm^{-1})	12214	11660	12081
Center (nm)	818.72	857.61	827.74
Linear intensity	0.0796	0.0518	0.0481
Integral intensity	286	184	196
FWHM (cm^{-1})	3367	3331	3838
Center (cm^{-1})	9471	9340	9222
Center (nm)	1055.81	1070.63	1084.4
Linear intensity	0.0179	0.0146	0.0114
Integral intensity	44	34	23
FWHM (cm^{-1})	2320	2183	1914

4) Corundum GRR 3473 from Queensland, Australia

Supplemental Table 4a. Selected major and trace element XRF analysis for GRR3473 corundum samples from Queensland, Australia, given in weight percent.

Sample	Fe_2O_3	TiO_2	MgO	Cr_2O_3	SiO_2
GRR3473-YS-D	2.605	N/A	N/A	N/A	0.110
GRR3473-GS-A	1.282	N/A	N/A	N/A	0.069
GRR3473-BS-A	1.576	0.154	N/A	N/A	0.136
GRR3473-BS-B	1.869	0.175	N/A	N/A	0.092

Many samples from this locality with sample number 3473 were initially screened. The labels "YS", "GS", and "BS" were used to distinguish between different sample archetypes.

"YS" designated samples with high Fe content where optical absorption spectra showed evidence of significant Fe^{3+} and comparatively low IVCT pair concentrations.

"GS" designated samples where the contribution of IVCT to the optical absorption spectrum was significant but either no Ti was measured, or the presence of Ti was questionable.

"BS" designated samples where IVCT was significant in the optical absorption spectra and the presence of Ti was more definitive based on XRF data.

Supplemental Table 4b. Additional Fe/Fe dominant corundum samples used in corroborating heating runs not included in main text.

Sample	Mineral	Locality	Thickness	Variety
GRR 3473-BS-A	Corundum	Queensland, Australia	1.016 mm	Fe/Fe IVCT (880 nm)-blue
GRR 3473-BS-B	Corundum	Queensland, Australia	0.683 mm	Fe/Fe IVCT (880 nm)-blue

Corundum GRR 3473-GS-A from Queensland, Australia

Supplemental Table 4c. Gaussian components with half-widths compatible at room temperature with IVCT band assignments in GRR3473-GS-A corundum.

	23 °C Start	500 °C Heat	1000 °C Heat
Center (cm^{-1})	23313	23097	22838
Center (nm)	428.94	432.95	437.87
Linear intensity	0.1971	0.2761	0.3373
Integral intensity	793	1535	2548
FWHM (cm^{-1})	3780	5222	7096
Center (cm^{-1})	18232	17941	16201
Center (nm)	548.48	557.38	617.25
Linear intensity	0.2786	0.2138	0.1766
Integral intensity	2016	1323	1178
FWHM (cm^{-1})	6798	5816	6264
Center (cm^{-1})	13368	14184	N/A
Center (nm)	748.05	705.04	N/A
Linear intensity	0.2865	0.1375	0
Integral intensity	1376	638	0
FWHM (cm^{-1})	4512	4360	N/A

Supplemental Table 4d. Gaussian components for broad feature in GRR3473-GS-A corundum with some *d-d* character, subject to additional splitting at elevated temperatures.

	23 °C Start	500 °C Heat	1000 °C Heat
Center (cm^{-1})	11023	11988	12298
Center (nm)	907.21	834.14	813.17
Linear intensity	0.7836	0.1086	0.0938
Integral intensity	2868	401	451
FWHM (cm^{-1})	3438	3468	4512
Center (cm^{-1})	N/A	10205	9825
Center (nm)	N/A	979.91	1017.82
Linear intensity	0	0.1123	0.0846
Integral intensity	0	323	291
FWHM (cm^{-1})	N/A	2704	3231
Barycenter (cm^{-1})	N/A	10918	10814
Barycenter (nm)	N/A	915.89	924.73
Combined integral intensity	2868	724	742

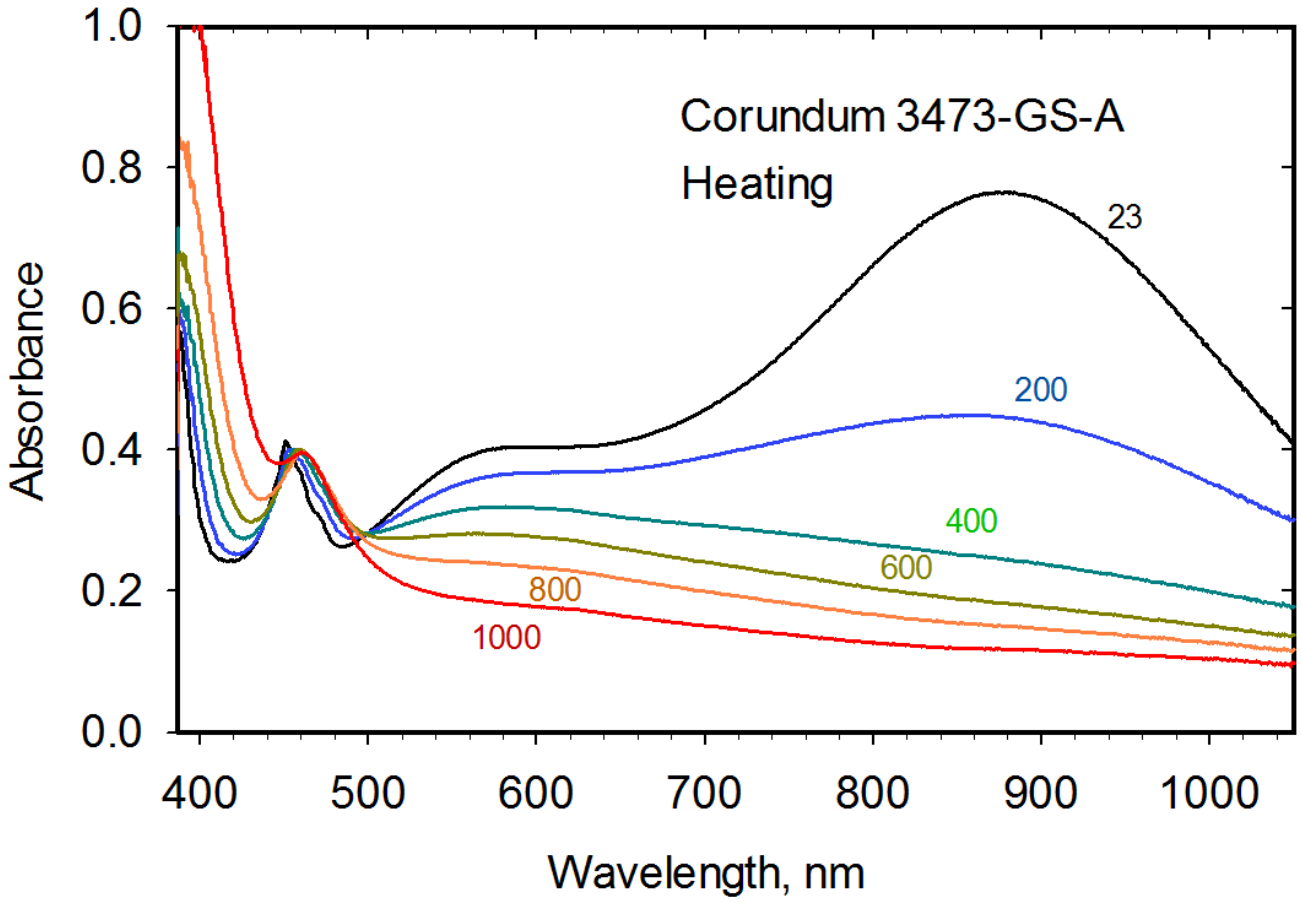

Supplemental Figure 4-GS-A-1. Initial heating run from 23 °C to 1000 °C of GRR3473-GS-A corundum from Queensland, Australia, presented as 1.000 mm thick showing the near complete loss of the IVCT bands at elevated temperatures.

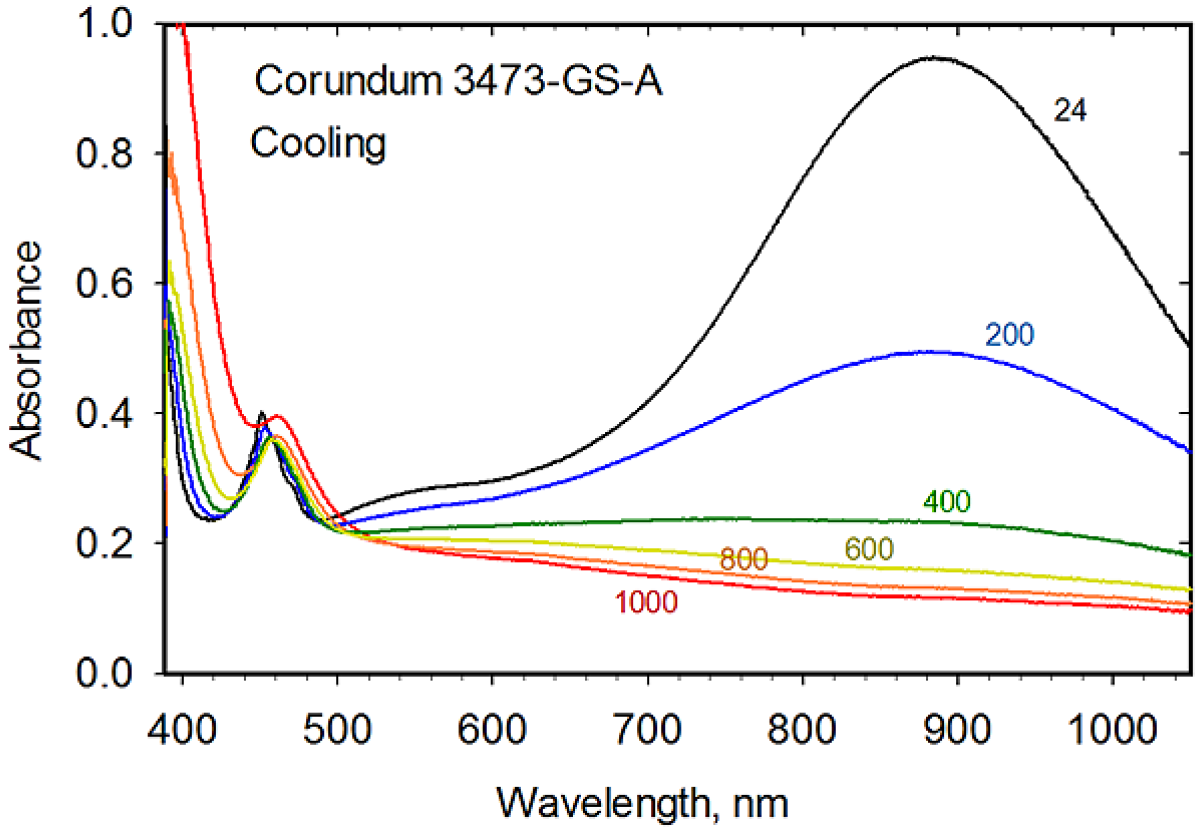

Supplemental Figure 4-GS-A-2. Initial cooling run of GRR3473-GS-A corundum from Queensland, Australia, presented as 1.000 mm thick. On recovery, the ~907 nm Fe/Fe IVCT feature increases in intensity asymmetrically towards longer wavelengths while the Fe/Ti IVCT feature decreases in intensity.

Corundum GRR 3473-BS-A from Queensland, Australia

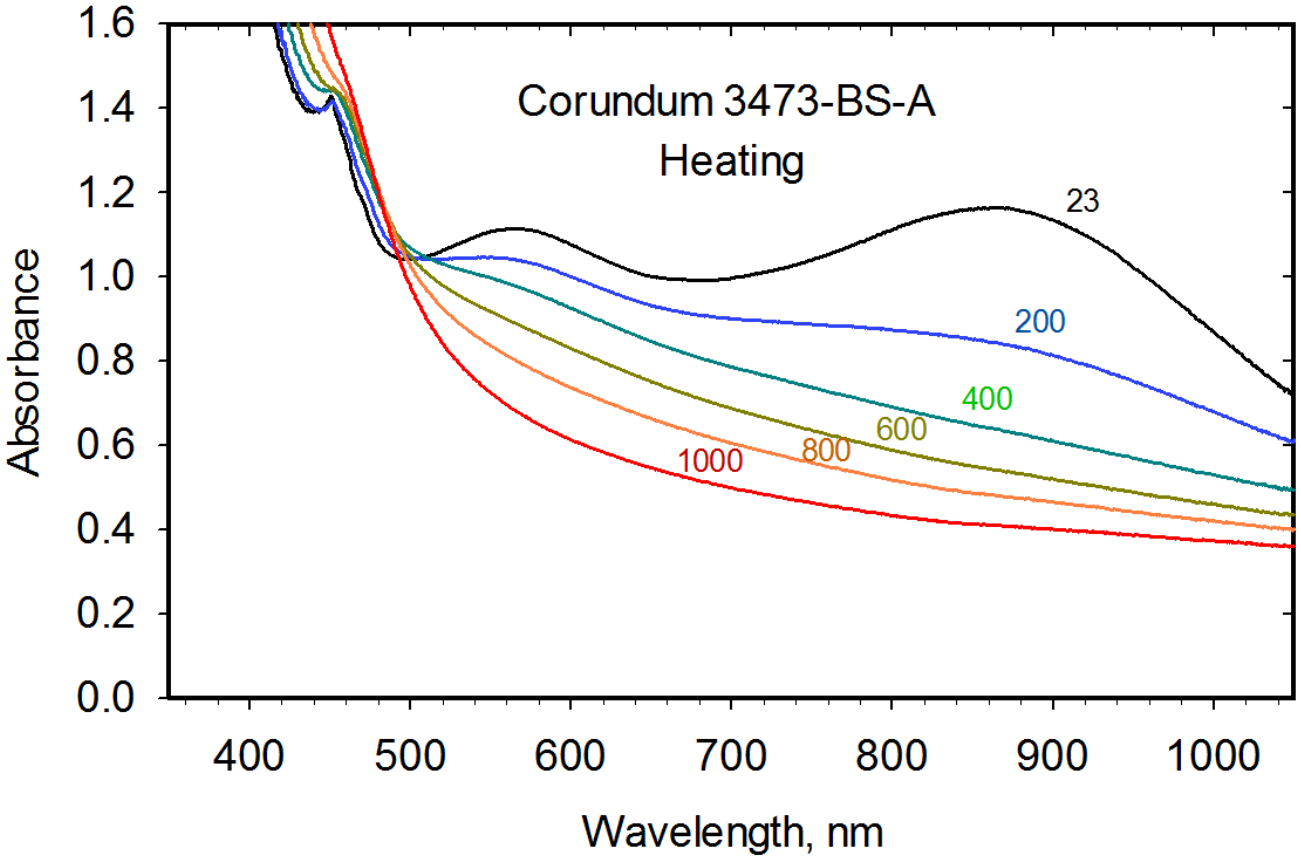

Supplemental Figure 4-BS-A-1. Initial heating run from 23 °C to 1000 °C of GRR3473-BS-A corundum from Queensland, Australia, presented as 1.000 mm thick.

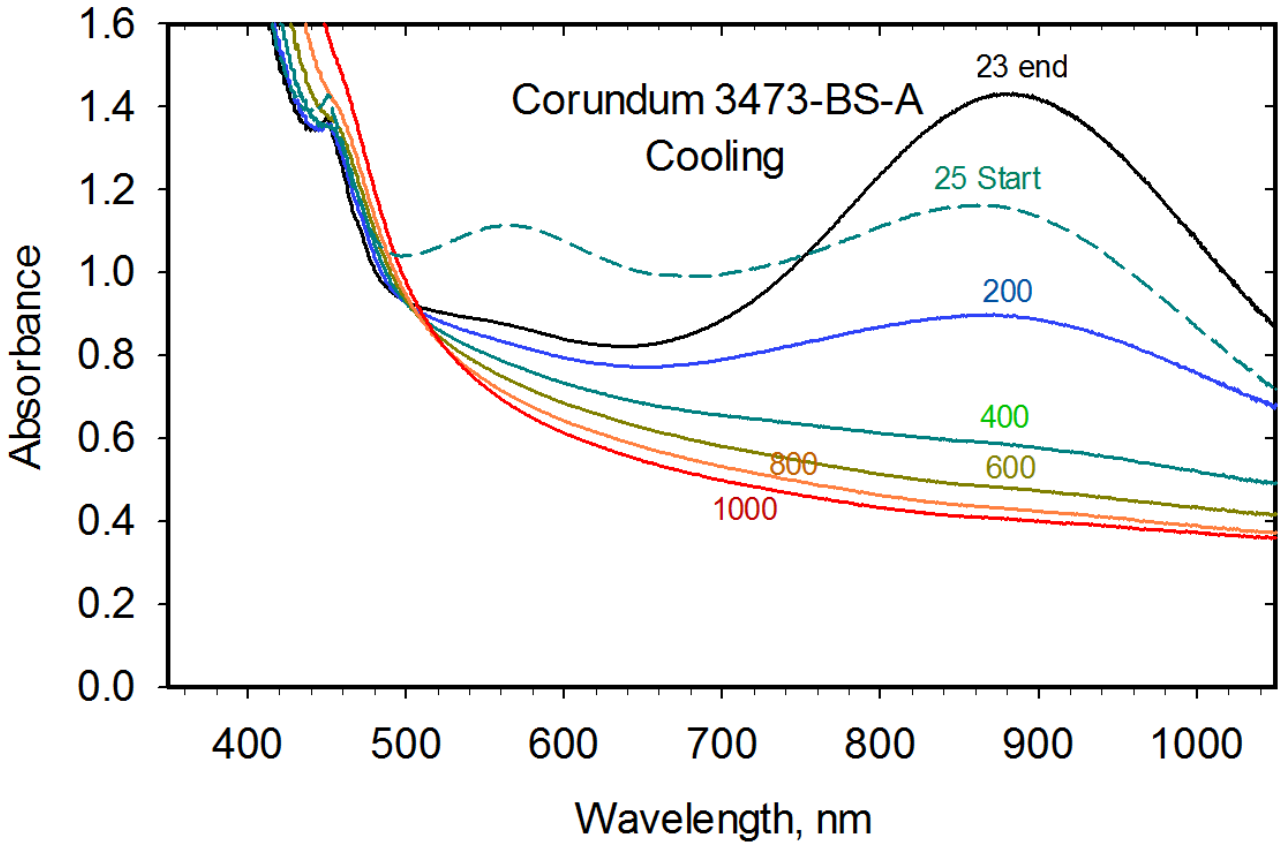

Supplemental Figure 4-BS-A-2. Initial cooling run of corundum GRR3473-BS-A from Queensland, Australia, presented as 1.000 mm thick. Similar changes are observed in recovery for the IVCT features as in other Fe/Fe IVCT dominant corundum samples.

Corundum GRR 3473-BS-B from Queensland, Australia

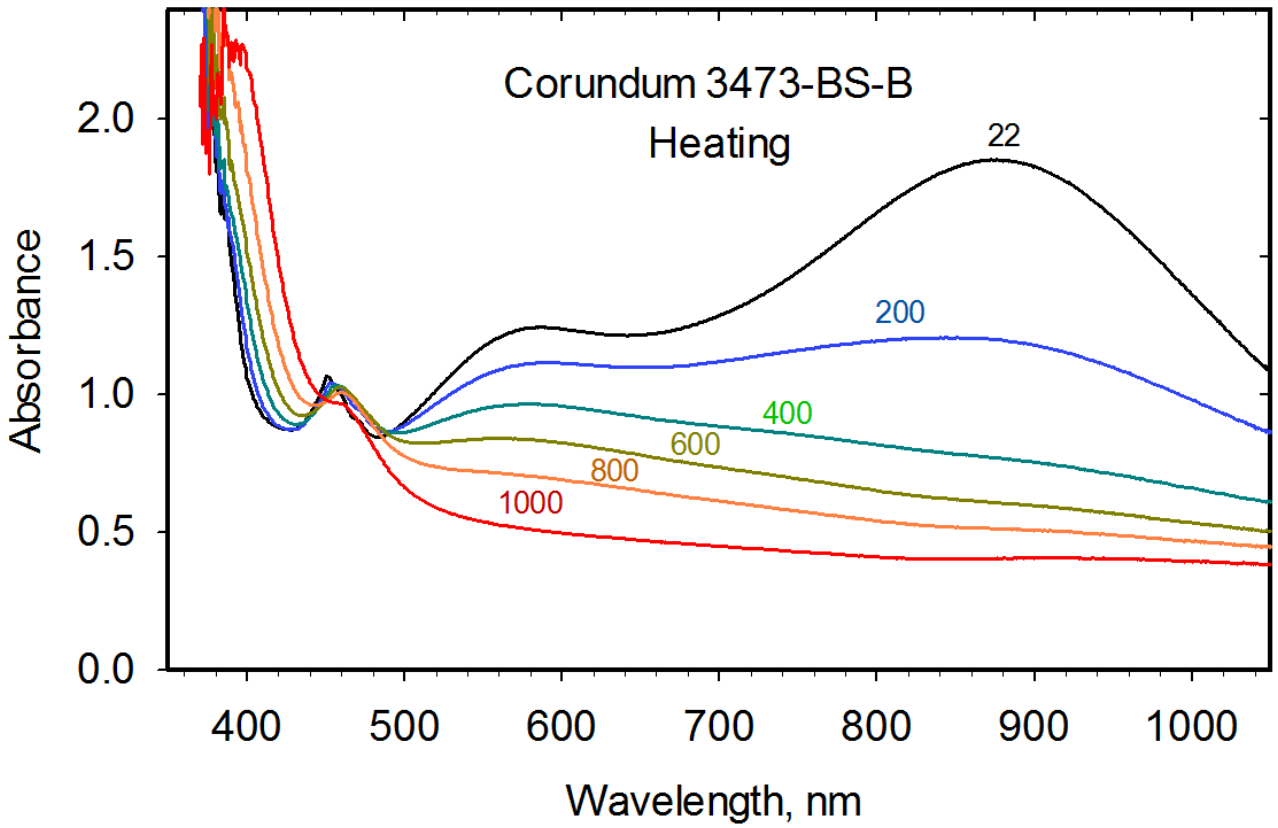

Supplemental Figure 4-BS-B-1. Initial heating run from 22 °C to 1000 °C of corundum GRR3473-BS-B from Queensland, Australia, presented as 1.00 mm thick.

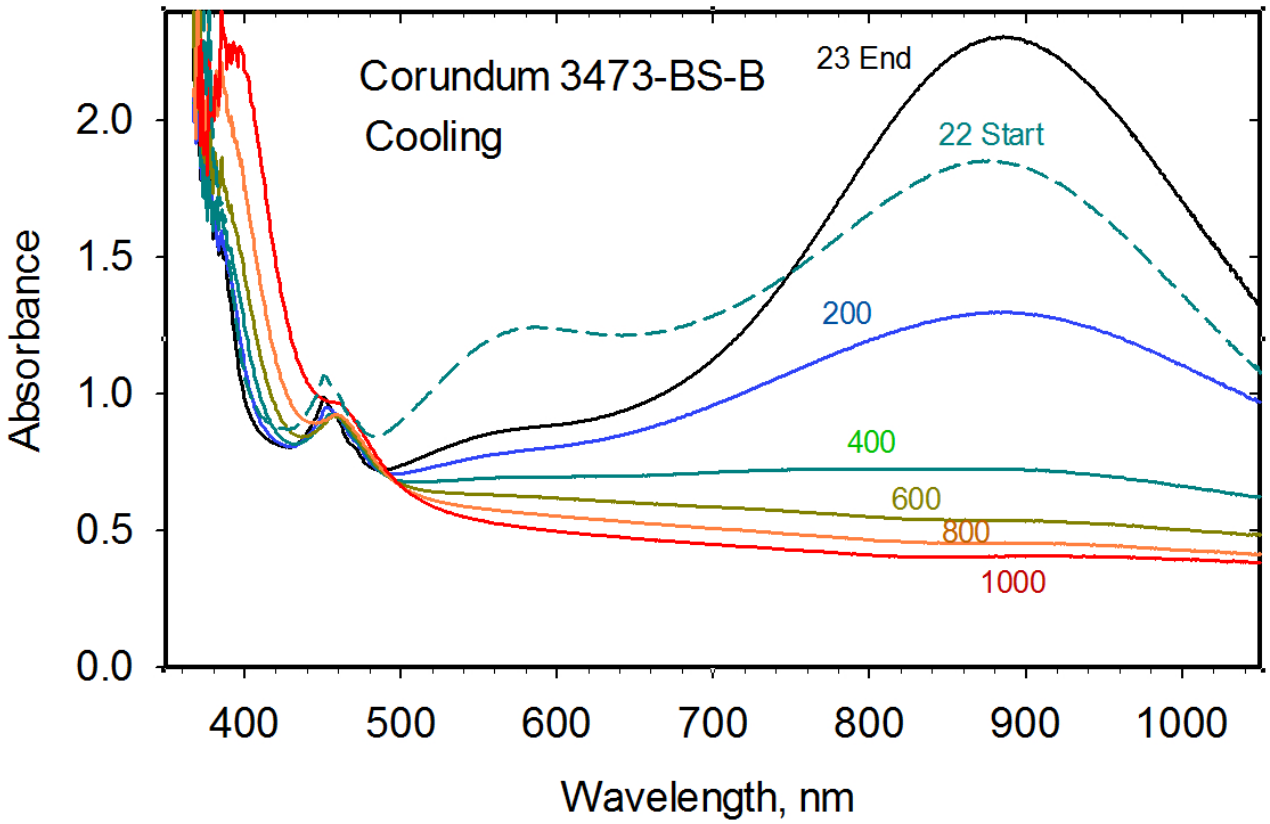

Supplemental Figure 4-BS-B-2. Initial cooling run from of corundum GRR3473-BS-B from Queensland, Australia, presented as 1.00 mm thick. Similar changes are observed in recovery for the IVCT features as in other Fe/Fe IVCT dominant corundum samples.

Al_2SiO_5 polymorphs (IVCT) supplemental figures

5) Kyanite GRR 285 from Minas Gerais, Brazil

Supplemental Table 5a. Parameters for Gaussian components compatible with IVCT assignments in GRR285 kyanite.

	23 °C Start	500 °C Heat	1000 °C Heat	25 °C End
Center (cm^{-1})	23303	24167	N/A (UV edge)	23590
Center (nm)	429.13	413.79	N/A (UV edge)	423.91
Linear intensity	0.0419	0.329	N/A (UV edge)	0.0846
Integral intensity	169	3270	N/A (UV edge)	477
FWHM (cm^{-1})	3791	9338	N/A (UV edge)	5294
Center (cm^{-1})	16379	16510	15843	16555
Center (nm)	610.52	605.69	631.2	604.03
Linear intensity	0.2394	0.2337	0.1332	0.2424
Integral intensity	1454	1485	957	1484
FWHM (cm^{-1})	5705	5970	6749	5751
Center (cm^{-1})	12186	13256	12076	12548
Center (nm)	820.62	754.39	828.1	796.94
Linear intensity	0.0658	0.0558	0.0175	0.0607
Integral intensity	221	224	69	222
FWHM (cm^{-1})	3156	3764	3715	3429

Supplemental Table 5b. Parameters for Gaussian components compatible with *d-d* assignments at room temperature in GRR285 kyanite.

	23 °C Start	500 °C Heat	1000 °C Heat	25 °C End
Center (cm^{-1})	16024	N/A	N/A	15973
Center (nm)	610.52	N/A	N/A	604.03
Linear intensity	0.0089	N/A	N/A	0.0119
Integral intensity	13	N/A	N/A	20
FWHM (cm^{-1})	1372	N/A	N/A	1580
Center (cm^{-1})	N/A	11531	N/A	11349
Center (nm)	N/A	867.22	N/A	881.13
Linear intensity	N/A	0.0275	N/A	0.0153
Integral intensity	N/A	68	N/A	34
FWHM (cm^{-1})	N/A	2329	N/A	2089

6) Silllimanite GRR 2020 from Mogok, Myanmar

Supplemental Table 6a. Gaussian components compatible at room temperature with IVCT band assignments in GRR2020 sillimanite.

	23 °C Start	300 °C Heat	500 °C Heat	1000 °C Heat
Center (cm^{-1})	23248	22921	21276	N/A (UV edge)
Center (nm)	430.14	436.28	470.02	N/A (UV edge)
Linear intensity	0.2483	0.2971	0.3629	N/A (UV edge)
Integral intensity	1995	1436	2668	N/A (UV edge)
FWHM (cm^{-1})	7549	4540	6908	N/A (UV edge)
Center (cm^{-1})	16887	16734	16337	17492
Center (nm)	592.18	597.6	612.11	571.69
Linear intensity	0.4494	0.4583	0.3402	0.3271
Integral intensity	2154	2124	1813	1910
FWHM (cm^{-1})	4503	4354	5006	5483

Supplemental Table 6b. Gaussian components that have parameters incompatible with IVCT but may nonetheless represent an IVCT band in GRR2020 sillimanite.

	23 °C Start	300 °C Heat	500 °C Heat	1000 °C Heat
Center (cm^{-1})	12651	12736	12529	13779
Center (nm)	790.44	785.18	798.14	725.76
Linear intensity	0.1618	0.1383	0.0958	0.1021
Integral intensity	473	446	300	413
FWHM (cm^{-1})	2747	3030	2938	3801
Center (cm^{-1})	11198	10965	10860	11683
Center (nm)	893.03	911.97	920.81	855.93
Linear intensity	0.0694	0.0434	0.0292	0.0318
Integral intensity	149	91	56	93
FWHM (cm^{-1})	2017	1977	1793	2737
Barycenter (cm^{-1})	11779	11674	11528	12521
Barycenter (nm)	848.96	856.64	867.48	798.64
Combined integral intensity	622	537	355	506

Supplemental Table 6c. Selected parameters for Gaussian components compatible with *d-d* assignments at room temperature in GRR2020 sillimanite.

	23 °C Start	300 °C Heat	500 °C Heat	1000 °C Heat
Center (cm^{-1})	20630	20268	N/A	N/A
Center (nm)	484.72	493.38	N/A	N/A
Linear intensity	0.0743	0.1623	0	0
Integral intensity	124	447	0	0
FWHM (cm^{-1})	1563	2588	N/A	N/A
Center (cm^{-1})	19173	18742	18608	N/A
Center (nm)	521.57	533.56	537.39	N/A
Linear intensity	0.0557	0.0934	0.0306	0
Integral intensity	81	192	66	0
FWHM (cm^{-1})	1361	1933	2028	N/A
Center (cm^{-1})	16214	N/A	N/A	N/A
Center (nm)	616.76	N/A	N/A	N/A
Linear intensity	0.0962	0	0	0
Integral intensity	164	0	0	0
FWHM (cm^{-1})	1596	N/A	N/A	N/A

7) Andalusite. GRR 375 from Tenderfoot Mountain, South Dakota

Supplemental Table 7a. Parameters for Gaussian components compatible with IVCT assignments at room temperature in GRR375 andalusite.

	24 °C Start (Run 1)	24 °C Start (Run 2)
Center (cm^{-1})	21312	21034
Center (nm)	469.21	475.43
Linear intensity	1.1029	0.5539
Integral intensity	7181	2559
FWHM (cm^{-1})	6117	4340
Center (cm^{-1})	16224	16877
Center (nm)	616.37	592.51
Linear intensity	0.2995	0.2932
Integral intensity	1802	2031
FWHM (cm^{-1})	5653	6507

Supplemental Table 7b. Parameters for Gaussian components compatible with *d-d* assignments at room temperature in GRR375 andalusite.

	24 °C Start (Run 1)	24 °C Start (Run 2)
Center (cm^{-1})	19490	19470
Center (nm)	513.08	513.6
Linear intensity	0.1537	0.1296
Integral intensity	352	301
FWHM (cm^{-1})	2150	2183
Center (cm^{-1})	18480	18487
Center (nm)	541.14	540.93
Linear intensity	0.1021	0.0579
Integral intensity	158	89
FWHM (cm^{-1})	1455	1447
Center (cm^{-1})	11010	11115
Center (nm)	908.29	899.7
Linear intensity	0.0172	0.0082
Integral intensity	21	14
FWHM (cm^{-1})	1127	1579

Octahedral Cr^{3+} & V^{3+} (*d-d*) supplemental figures and data

8) Corundum, variety ruby, GRR 1843 from Myanmar

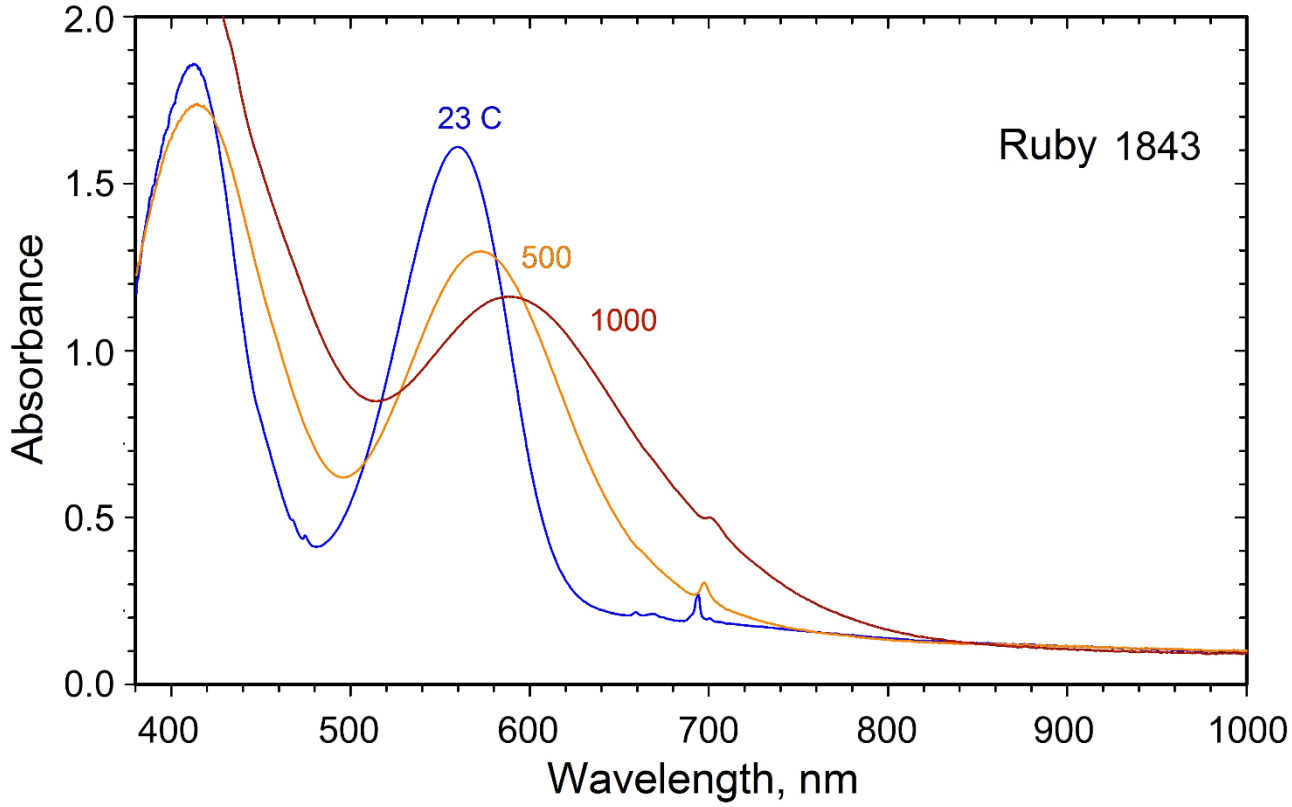

Supplemental Figure 8. The temperature dependence of the E⊥c spectrum of ruby GRR 1843 from Myanmar, dominated by Cr^{3+} spin-allowed *d-d* bands, presented as 1.00 mm thick.

9) Kyanite:Cr^{3+} GRR 656 from Transvaal, South Africa

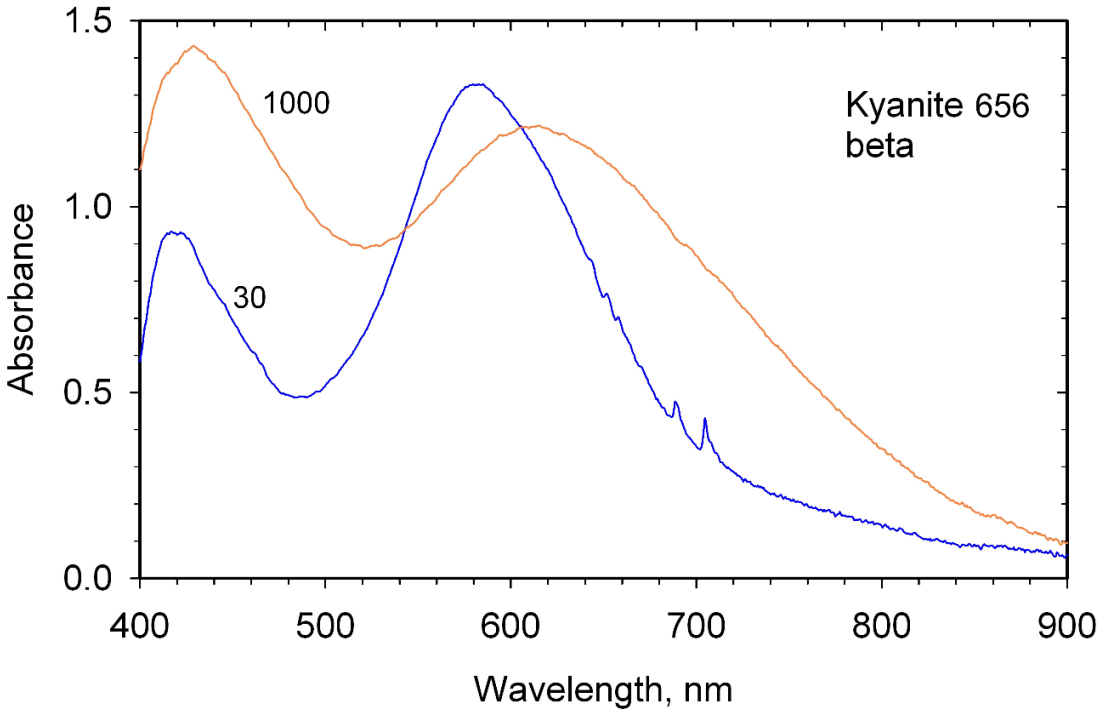

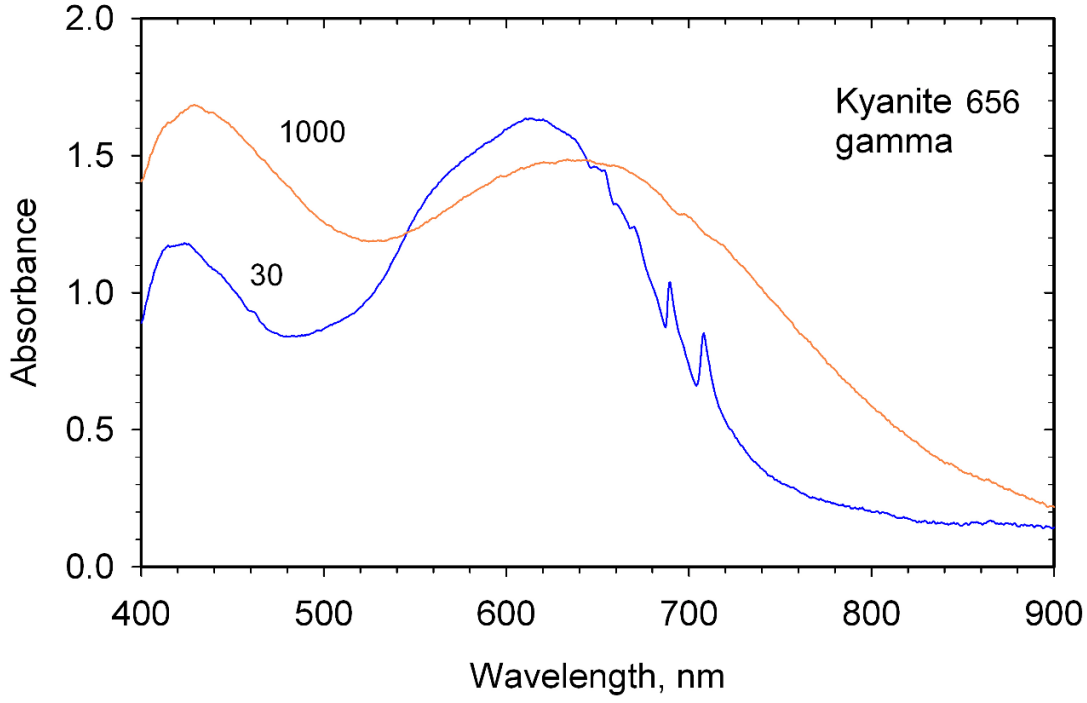

Supplemental Figures 9a, 9b. Variable temperature spectra of chromium-containing kyanite GRR 656 in E||β and E||γ, plotted for 1.00 mm thickness.

10) Spinel:V^{3+} GRR 656 from Nam Ya, Myanmar

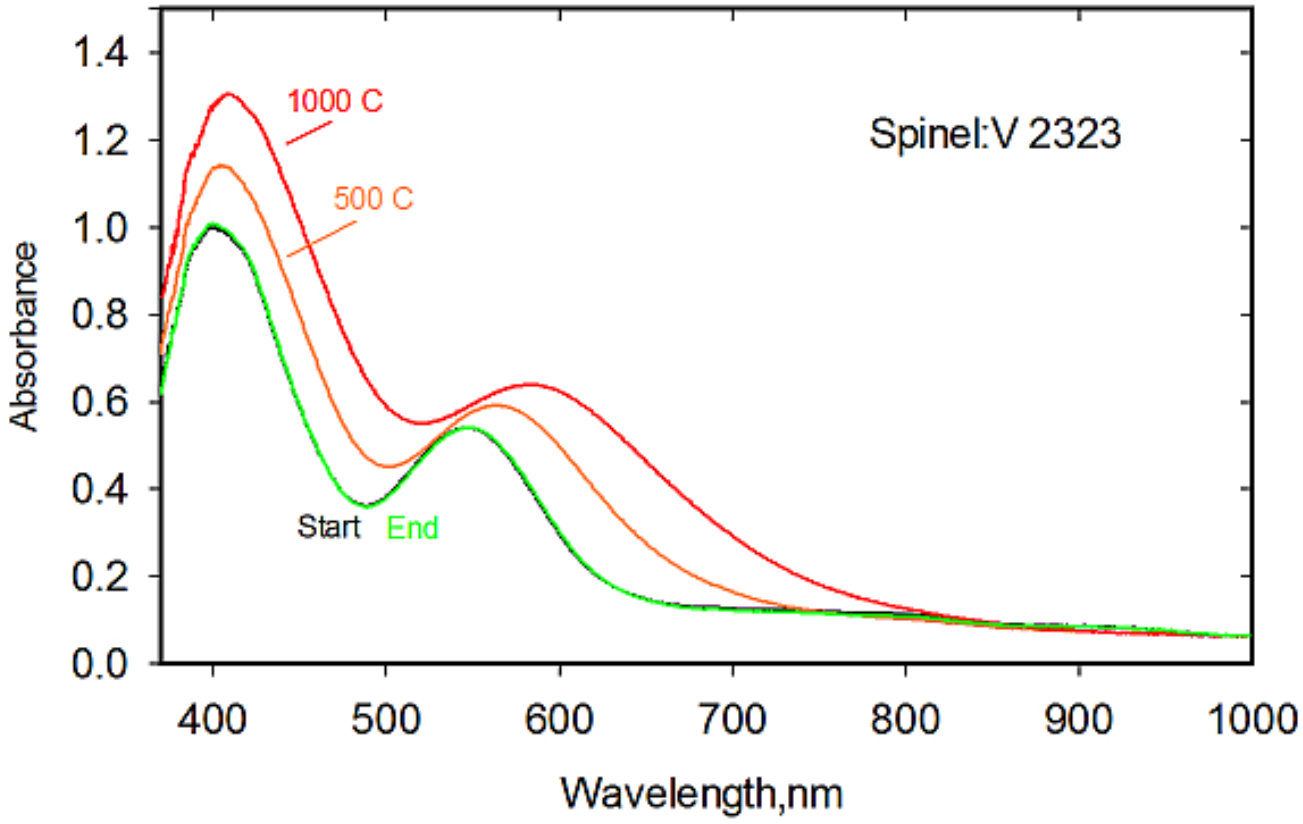

Supplemental Figure 10. Spectrum of V^{3+}-dominant spinel GRR 2323 from Myanmar presented as 1.000 mm thick. Spin-allowed band intensities increase at temperature due to vibronic coupling and completely recover when cooled.

Fe/Ti IVCT supplemental tables

Supplemental Table 11. Comparison of ~570-575 nm Fe/Ti IVCT band parameters in 1000 °C sillimanite and room temperature Fe/Ti dominant corundum.

Sample	Sillimanite 2020-D	Corundum 2382-B
Temperature	1000 °C Heat	24 °C Start
Center (cm^{-1})	17492	17401
Center (nm)	571.69	574.67
Linear intensity	0.3271	0.2867
Integral intensity	1910	1648
FWHM (cm^{-1})	5483	5400

Supplemental Table 12. Comparison of Fe/Ti IVCT band parameters in Fe/Fe dominant corundum at room and moderate heating temperatures to Fe/Ti dominant corundum at room temperature.

Sample	Fe/Fe Corundum (GRR3473-GS-A)		Fe/Ti Corundun (GRR2382-B)
Temperature	23 °C Start	500 °C Heat	24 °C Start
Center (cm^{-1})	18232	17941	17401
Center (nm)	548.48	557.38	574.67
Linear intensity	0.2786	0.2138	0.2867
Integral intensity	2016	1323	1648
FWHM (cm^{-1})	6798	5816	5400
---	---	---	---
Center (cm^{-1})	13368	14184	14134
Center (nm)	748.05	705.04	707.49
Linear intensity	0.2865	0.1375	0.0655
Integral intensity	1376	638	187
FWHM (cm^{-1})	4512	4360	2685

Supplemental Table 13. Comparison of Fe/Ti IVCT band parameters at 1000 °C in Fe/Fe dominant corundum and Fe/Ti dominant corundum.

Sample	Fe/Fe Corundum (GRR3473-GS-A)	Fe/Ti Corundum (GRR2382-B)
Temperature	1000 °C Heat	1000 °C Heat
Center (cm^{-1})	16201	16177
Center (nm)	617.25	618.18
Linear intensity	0.1766	0.0936
Integral intensity	1178	439
FWHM (cm^{-1})	6264	4408
Center (cm^{-1})	N/A	14154
Center (nm)	N/A	706.5
Linear intensity	0	0.0163
Integral intensity	0	40
FWHM (cm^{-1})	N/A	2274

Supplemental Table 14. Comparison of Fe/Ti band parameters in corundum and Al_2SiO_5 polymorphs. Band centers fall between 17000 and 16500 cm^{-1}.

Sample	Corundum 2382-B 500 °C	Sillimanite 2020-D	Andalusite 375 (Run 2)	Sillimanite 2020-D	Kyanite 285	Kyanite 285
Temperature	Heat	23 °C Start	24 °C Start	300 °C Heat	25 °C End	500 °C Heat
Center (cm^{-1})	16959	16887	16877	16734	16555	16510
Center (nm)	589.66	592.18	592.51	597.6	604.03	605.69
Linear intensity	0.0736	0.4494	0.2932	0.4583	0.2424	0.2337
Integral intensity	246	2154	2031	2124	1484	1485
FWHM (cm^{-1})	3148	4503	6507	4354	5751	5970

Supplemental Table 15. Comparison of Fe/Ti band parameters in corundum and Al_2SiO_5 polymorphs. Band centers fall between 16400 and 16100 cm^{-1}.

	Kyanite	Sillimanite	Andalusite	Corundum	Corundum
Sample	285	2020-D	375 (Run 1)	3473-GS-A	2382-B
Temperature	23 °C Start	500 °C Heat	24 °C Start	1000 °C Heat	1000 °C Heat
Center (cm^{-1})	16379	16337	16224	16201	16177
Center (nm)	610.52	612.11	616.37	617.25	618.18
Linear intensity	0.2394	0.3402	0.2995	0.1766	0.0936
Integral intensity	1454	1813	1802	1178	439
FWHM (cm^{-1})	5705	5006	5653	6264	4408

Supplemental Table 16. Comparison of broad bands at short wavelengths in Al_2SiO_5 polymorphs. Band centers fall between 24200 and 22900 cm^{-1}.

Sample	Kyanite 285	Kyanite 285	Kyanite 285	Sillimanite 2020-D	Sillimanite 2020-D
Temperature	500 °C Heat	25 °C End	23 °C Start	23 °C Start	300 °C Heat
Center (cm^{-1})	24167	23590	23303	23248	22921
Center (nm)	413.79	423.91	429.13	430.14	436.28
Linear intensity	0.329	0.0846	0.0419	0.2483	0.2971
Integral intensity	3270	477	169	1995	1436
FWHM (cm^{-1})	9338	5294	3791	7549	4540

Supplemental Table 17. Comparison of broad bands at short wavelengths in Fe/Ti corundum and Al_2SiO_5 polymorphs. Band centers fall between 21400 and 19400 cm^{-1}.

	Andalusite	Sillimanite	Andalusite	Corundum	Corundum
Sample	375 (Run 1)	2020-D	375 (Run 2)	2382-B	2382-B
Temperature	24 °C Start	500 °C Heat	24 °C Start	1000 °C Heat	500 °C Heat
Center (cm^{-1})	21312	21276	21034	20685	19409
Center (nm)	469.21	470.02	475.43	483.45	515.22
Linear intensity	1.1029	0.3629	0.5539	0.1637	0.1709
Integral intensity	7181	2668	2559	1011	858
FWHM (cm^{-1})	6117	6908	4340	5804	4714

Supplemental Table 18. Comparison of Fe/Ti band configuration for room temperature andalusite and 500 °C sillimanite.

Sample	Andalusite 375 (Run 1)	Sillimanite 2020-D
Temperature	24 °C Start	500 °C Heat
Center (cm^{-1})	21312	21276
Center (nm)	469.21	470.02
Linear intensity	1.1029	0.3629
Integral intensity	7181	2668
FWHM (cm^{-1})	6117	6908
---	---	---
Center (cm^{-1})	16224	16337
Center (nm)	616.37	612.11
Linear intensity	0.2995	0.3402
Integral intensity	1802	1813
FWHM (cm^{-1})	5653	5006

Fe/Fe IVCT supplemental figures

Supplemental Table 19. Calculation of octahedral barycenter in GRR285 kyanite between the Fe/Fe IVCT band and a lower energy component that has a compatible half-width with a *d-d* band assignment.

	23 °C Start	500 °C Heat	1000 °C Heat	25 °C End
Center (cm^{-1})	12186	13256	12076	12548
Center (nm)	820.62	754.39	828.1	796.94
Linear intensity	0.0658	0.0558	0.0175	0.0607
Integral intensity	221	224	69	222
FWHM (cm^{-1})	3156	3764	3715	3429
Center (cm^{-1})	N/A	11531	N/A	11349
Center (nm)	N/A	867.22	N/A	881.13
Linear intensity	N/A	0.0275	N/A	0.0153
Integral intensity	N/A	68	N/A	34
FWHM (cm^{-1})	N/A	2329	N/A	2089
Barycenter (cm^{-1})	N/A	12221	N/A	11829
Barycenter (nm)	N/A	818.26	N/A	845.4
Combined integral intensity	N/A	292	N/A	256

Supplemental Table 20. Comparison of Fe/Fe IVCT band parameters in Fe/Fe dominant corundum and Al_2SiO_5 polymorphs at selected elevated temperatures to Fe/Ti dominant corundum at room temperature. Includes calculation of octahedral barycenters across components for each sample.

	Kyanite	Sillimanite	Sillimanite	Fe/Fe Corundum	Fe/Ti Corundum
Sample	285	2020-D	2020-D	(GRR3473-GS-A)	(GRR2382-B)
Temperature	500 °C Heat	500 °C Heat	1000 °C Heat	1000 °C Heat	24 °C Start
Center (cm^{-1})	13256	12529	13779	12298	12214
Center (nm)	754.39	798.14	725.76	813.17	818.72
Linear intensity	0.0558	0.0958	0.1021	0.0938	0.0796
Integral intensity	224	300	413	451	286
FWHM (cm^{-1})	3764	2938	3801	4512	3367
Center (cm^{-1})	11531	10860	11683	9825	9471
Center (nm)	867.22	920.81	855.93	1017.82	1055.81
Linear intensity	0.0275	0.0292	0.0318	0.0846	0.0179
Integral intensity	68	56	93	291	44
FWHM (cm^{-1})	2329	1793	2737	3231	2320
Barycenter (cm^{-1})	12221	11528	12521	10814	10569
Barycenter (nm)	818.26	867.48	798.64	924.73	946.2
Combined integral intensity	292	355	506	742	330

Supplemental Table 21. Comparison of Fe/Fe IVCT band parameters in Fe/Fe dominant and Fe/Ti dominant corundum throughout heating, including calculation of octahedral barycenters across components in both samples.

Sample	Fe/Fe Corundum GRR3473-GS-A			Fe/Ti Corundum GRR2382-B		
Temperature	23 °C Start	500 °C Heat	1000 °C Heat	24 °C Start	500 °C Heat	1000 °C Heat
Center (cm^{-1})	11023	11988	12298	12214	11660	12081
Center (nm)	907.21	834.14	813.17	818.72	857.61	827.74
Linear intensity	0.7836	0.1086	0.0938	0.0796	0.0518	0.0481
Integral intensity	2868	401	451	286	184	196
FWHM (cm^{-1})	3438	3468	4512	3367	3331	3838
Center (cm^{-1})	N/A	10205	9825	9471	9340	9222
Center (nm)	N/A	979.91	1017.82	1055.81	1070.63	1084.4
Linear intensity	0	0.1123	0.0846	0.0179	0.0146	0.0114
Integral intensity	0	323	291	44	34	23
FWHM (cm^{-1})	N/A	2704	3231	2320	2183	1914
Barycenter (cm^{-1})	N/A	10918	10814	10569	10268	10365
Barycenter (nm)	N/A	915.89	924.73	946.2	973.87	964.75
Combined integral intensity	2868	724	742	330	217	220

Sample Supplemental Documentation

Prior to conducting heating runs, decomposition temperatures at standard pressure (1 atm) were investigated for all mineral types used in this study; literature values were all found to be above 1000 °C, so this temperature was applied as a common upper limit across all samples.

It is also possible for inclusions or minor co-occurring mineral phases to be altered at high temperatures. Among tested samples, sillimanite was the main one where such effects may have been relevant. Sillimanite samples from the GRR2020 catalog number occur with a dull yellow-orange mineral phase. After heating the specific sample that was used in this study, parts of the sample turned a dark brown to black color. Rossman et al (1982) previously noted inclusions with a similar description in sillimanite samples: they find that brown sillimanite contains “acicular inclusions of opaque or dark brown material, presumably an Fe or Fe – Ti oxide.” Despite the observed visual change in the sample, limited to no change occurs in its room temperature absorption spectrum.

In minerals, rapid heating and cooling can cause physical damage such as cracking. The two minute delays at every 100 °C interval in heating and cooling were primarily implemented to allow more than adequate time for thermal equilibration to each new measurement temperature, as discussed in the experimental section. These delays were likely also helpful in reducing the effects of thermal shock. In general, limited to no observable physical damage occurred. Corundum has been observed previously to be highly resistant to fracturing induced by thermal shock during heat treatment (Emmett and Douthit 1993). Some changes were noted in the GRR285 kyanite sample: minor black discoloration occurred along the edges of the sample where it had been cut to fit the dimensions required by the temperature stage.

Corundum

GRR1843 Corundum

Variety ruby. Purchased in Chanthaburi, Thailand, but likely originally sourced from Myanmar. The coloration is due to its Cr^{3+} content.

GRR2382 Corundum

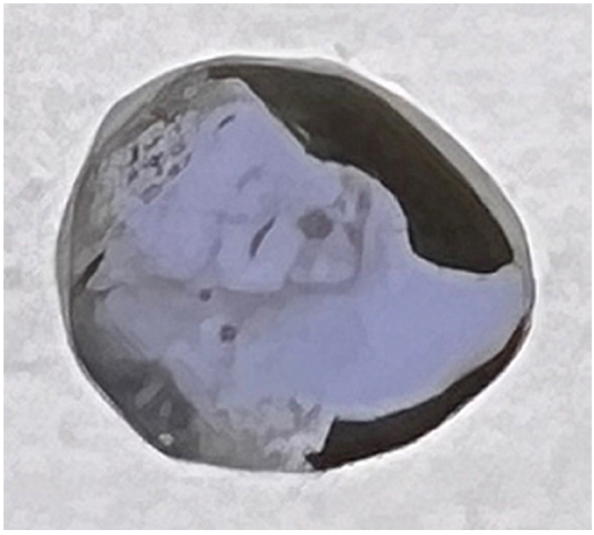

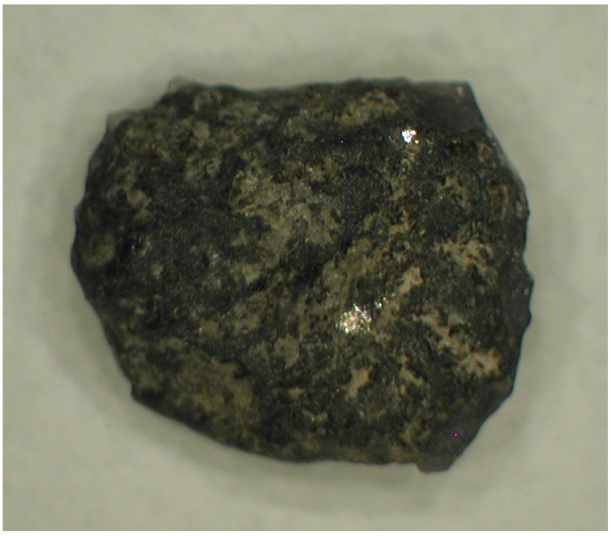

Left to right: Sample B used in heating runs; unprepared sample from this catalog number.

Variety sapphire. From Yogo Gulch in Judith Basin County, Montana, USA. This catalog number contains numerous 5 to 8 mm crystals.

The coloration of samples taken from the Yogo Gulch, MT locality is highly uniform. Samples with significant Cr^{3+} content will have a light purple tint; this is not the case for Sample B, which is a clear blue. The black sections on the sample are from a different mineral phase that occurs with the corundum.

GRR3473 Corundum

Variety sapphire. From Queensland, Australia. This catalog number contains several small pebbles.

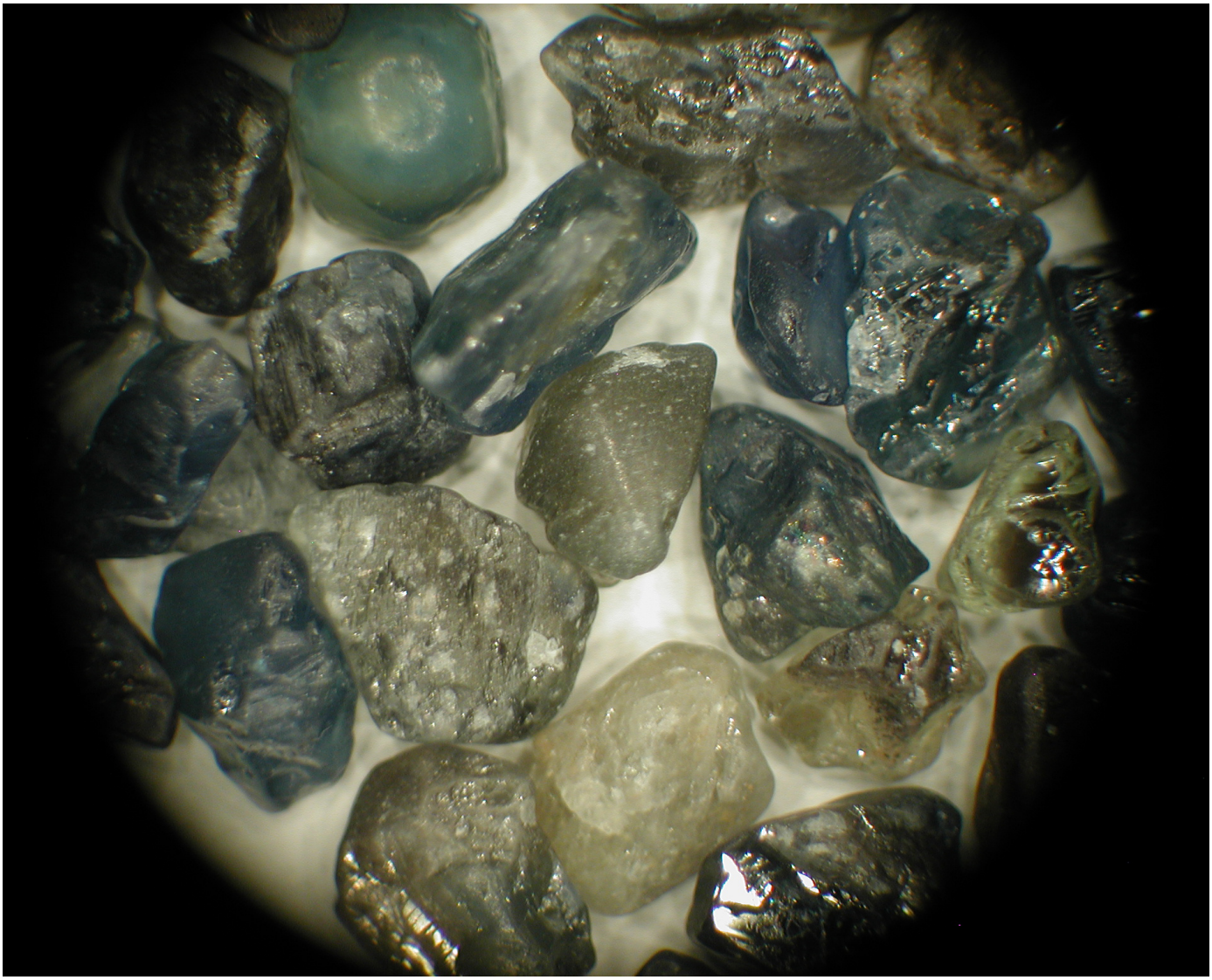

Corundum taken from this locality has relatively high iron content. Many samples with this catalog number are fairly turbid; their colors vary substantially from yellow to green to blue to black. Fe^{3+} content is the primary cause of color in yellow to yellow-green samples; IVCT is more significant in samples that display shades of blue.

The samples used that contain blue sections from IVCT are all zoned; cation diffusion during heating had a minor smearing effect on colors between zones for the GS-A, BS-A and BS-B samples.

YS-D

Bright yellowish green Fe^{3+} dominant corundum. Thin, dark brown stripes can be seen running through the sample. These are likely rutile (TiO_2) inclusions: fine needles have been observed previously in natural corundum samples with high Fe content from other localities (Emmett and Douthit 1991).

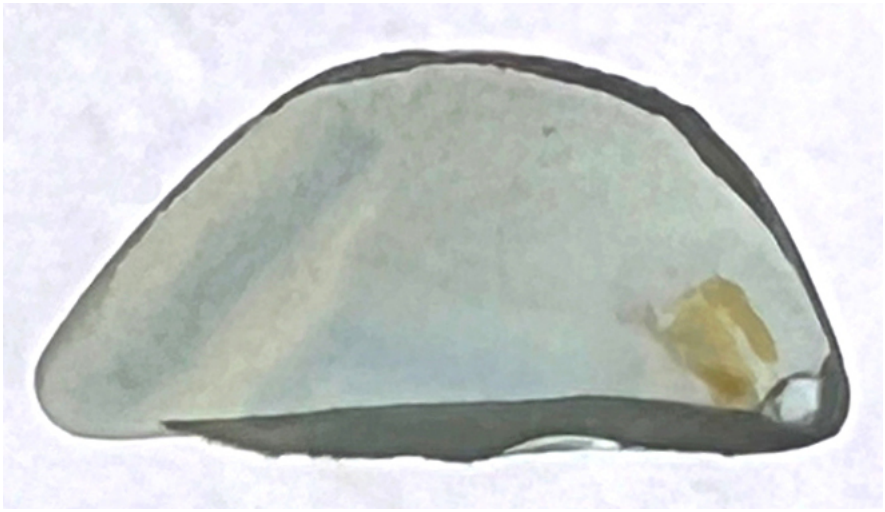

GS-A

Zoned IVCT sample containing sections of light blue and of pale yellow to yellow-green. One corner of the sample bears a small orange-brown inclusion.

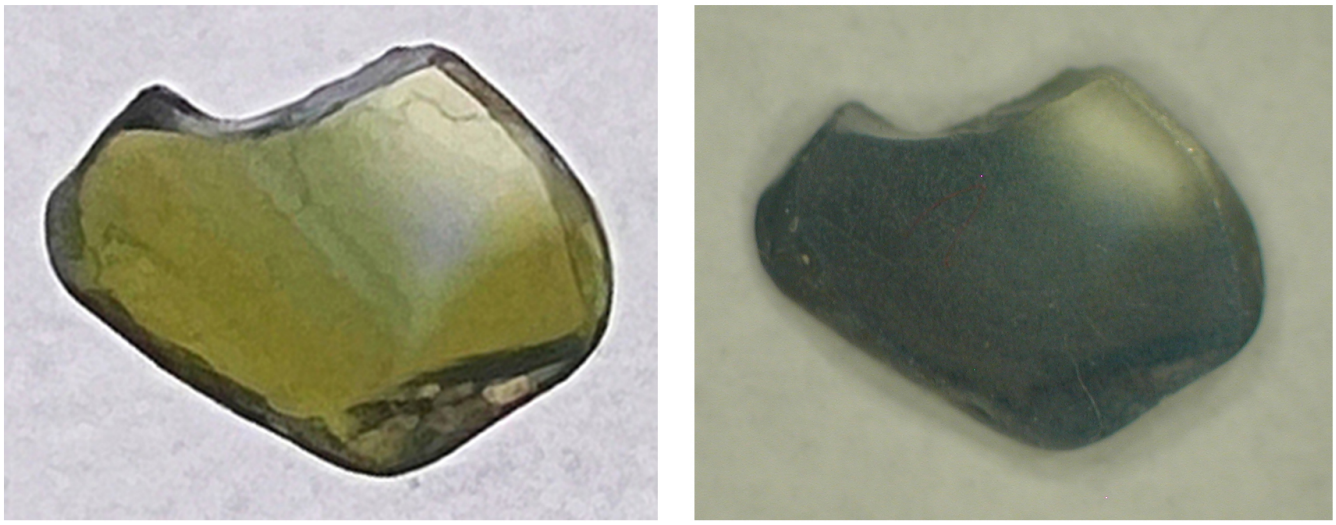

(same sample, photographed under different lighting conditions)

BS-A

Highly turbid and non-uniform IVCT sample. Colors are a mix of a bright blue and a brownish yellow-green. The relative visibility of the different colors varies depending on lighting.

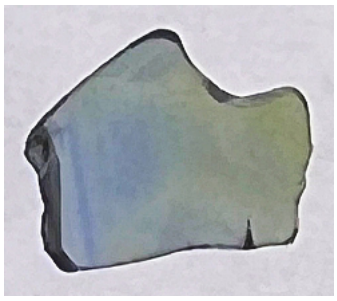

BS-B

Compared to the GS-A and BS-A samples, Sample BS-B was the darkest sample before being thinned during the preparation process for optical absorption studies. Zoned IVCT sample with blue sections in a hazy sea of brownish yellow-green.

Al_2SiO_5 polymorphs

GRR375 Andalusite

From Tenderfoot Mountain near Custer, Custer Co, South Dakota, USA.

The sample is highly non-uniform with numerous darker and lighter brown sections.

GRR285 Kyanite

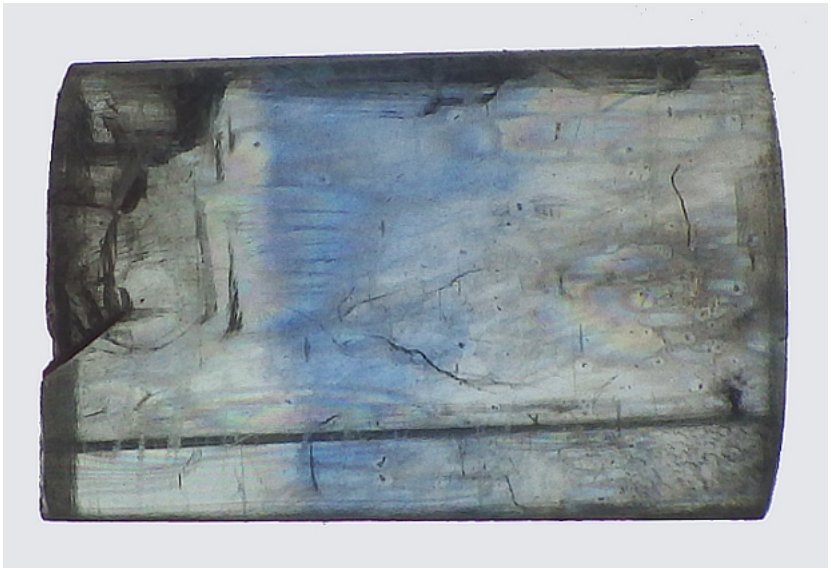

From Minas Gerais, Brazil.

Small piece cut from a larger cleavage slab. Strongly zoned. A blue streak runs through the center of the crystal; the blue color is due to IVCT.

GRR656 Kyanite

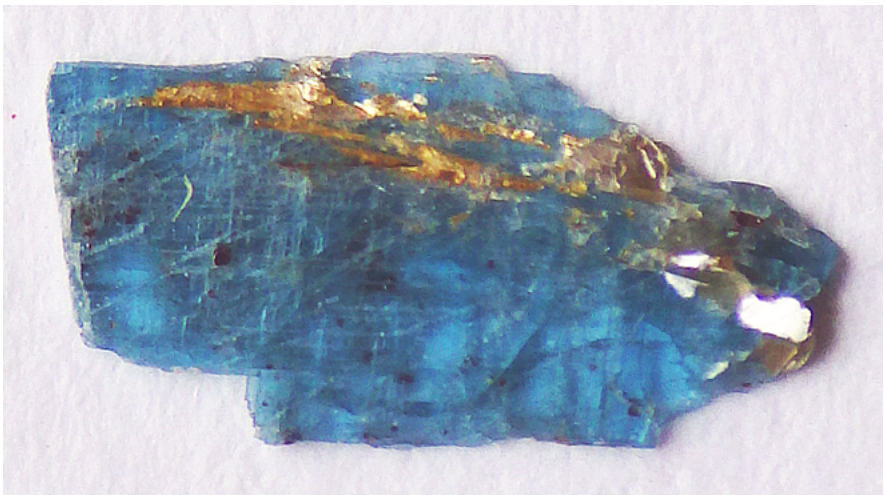

From Mashishimala Hills, Letaba District, Transvaal, South Africa.

Bright blue kyanite, occurring with fuchite. The blue here is primarily due to Cr^{3+} content rather than IVCT.

GRR2020 Sillimanite

From Mogok, Myanmar.

Though described as a blue fibrolite, most samples from this catalog number appear nearly colorless with at most a faint gray-blue tint. The dark brown to black sections in the photo above appear after heating.

Spinel

GRR2085 Spinel

From Mogok, Myanmar.

This catalog number contains assorted colors of spinel with a variety of chemical compositions in a jar of tumbled gem gravel. The Fe^{2+} spinel sample pictured here is a light purple color and contains reddish brown inclusions

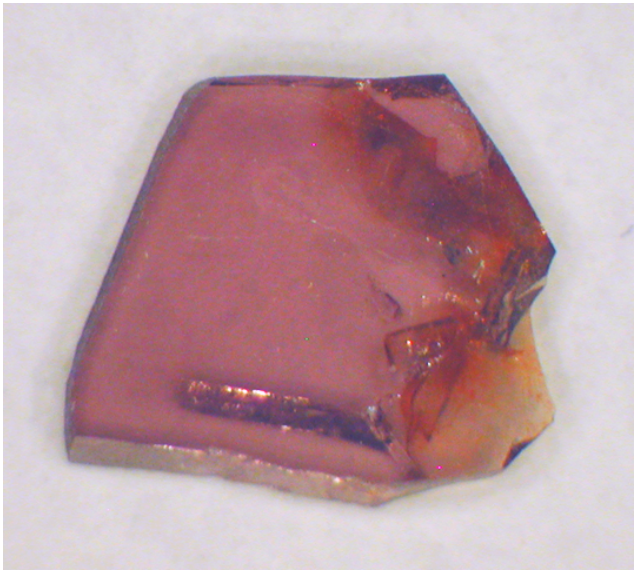

.

GRR2323 Spinel

From Namyazeik, Kachin State, Myanmar.

This catalog number corresponds to a box of pebbles, mostly spinel. The sample pictured here is a V^{3+} dominant spinel sample, though its Cr^{3+} content also contributes to the color – a pink to reddish pink.